UBIAT
REPORT
2024

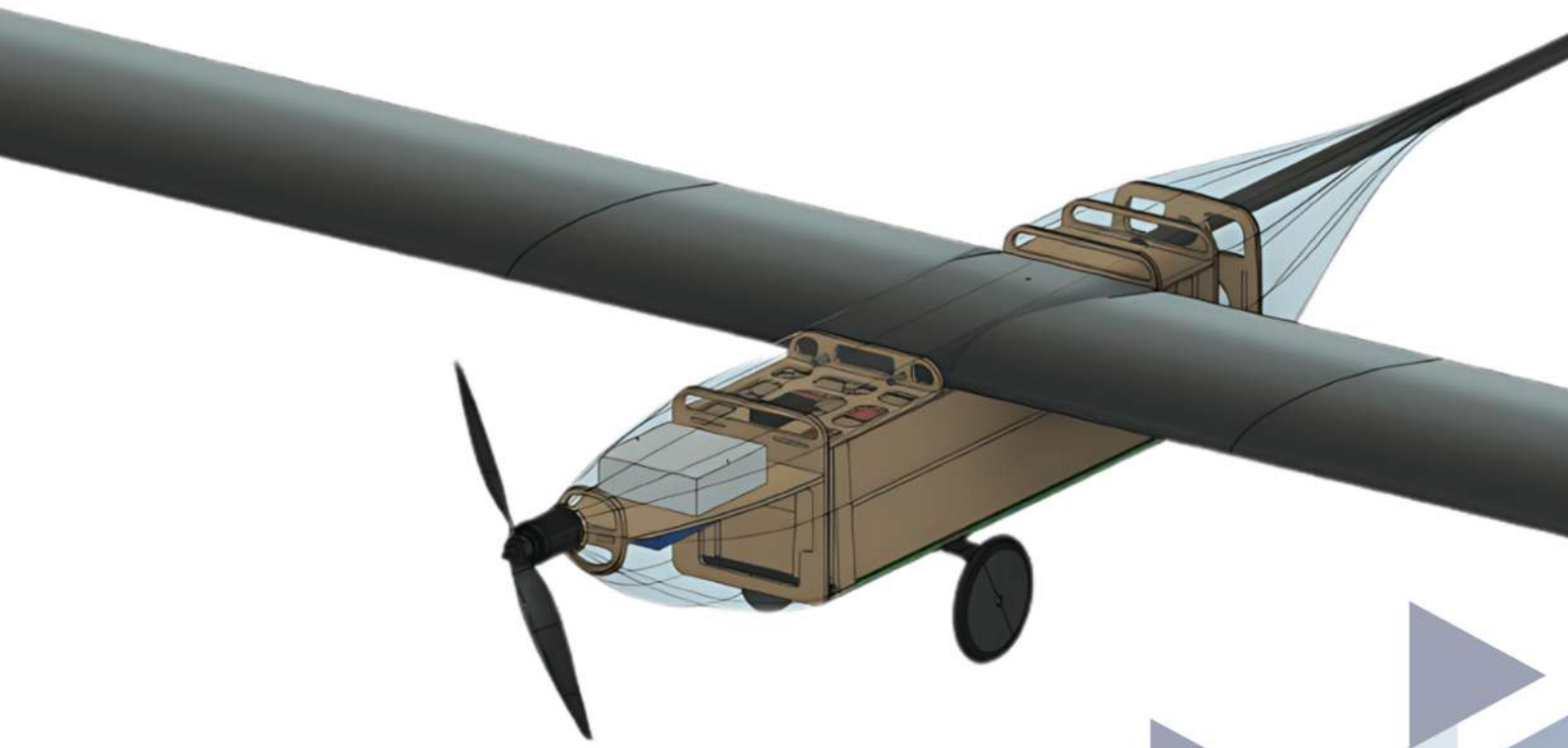

UBI AERONAUTICS TEAM (Team 05)

TECHNICAL REPORT FOR:
AIR CARGO CHALLENGE AACHEN 2024

Contents

1 Introduction

1.1 Objective and University History

This report summarizes the design of a small aircraft for payload transportation to compete in the ”Air Cargo Challenge” 2024 in Aachen, Germany, by a group of students from Universidade da Beira Interior, Portugal.

Universidade da Beira Interior (UBI), through the Department of Aerospace Sciences (DCA) and supported by multiple sponsors, has a notable track record in this competition.

Our victory in the inaugural 2003 edition led us to host the event in 2005. With three wins and two hosting events in 10 editions, our teams' past achievements fuel our determination to excel once more in this contest.

Edition	Year	Location	Organisation	Classification UBI
1^{st}	2003	Ota, Portugal	APAE	1^{st} place
2^{nd}	2005	Lisbon, Portugal	APAE	3^{rd} and 6^{th} places
3^{rd}	2007	Lisbon, Portugal	APAE and EUROAVIA	1^{st} and 7^{th} places
4^{th}	2009	Covilhã, Portugal	AS Covilhã	Organising team, 14^{th} place
5^{th}	2011	Stuttgart, Germany	AS Stuttgart and APAE	1^{st} place
6^{th}	2013	Ota, Portugal	AS Covilhã	Organising team
7^{th}	2015	Stuttgart, Germany	AS Stuttgart	5^{th} place
8^{th}	2017	Zagreb, Croatia	AS Zagreb	20^{th} and 23^{th} places
9^{th}	2019	Stuttgart, Germany	AS Stuttgart	5^{th} place
10^{th}	2022	Munich, Germany	AS Munich	13^{th} place

Table 1: History of Participation

1.2 UBI Aeronautics Team

The UBI Aeronautics Team was created in january of 2023 with the intent of participating in the 11^{th} and subsequent editions of Air Cargo Challenge, and is our objective that the team expands to other projects and competitions, in the aeronautics field, in the future.

In this years edition, our team in comprised of 29 students members from the 2^{nd} to the 3^{rd} years of the Bachelor's Degree in Aeronautical Engineering and an Integrated Master's student as our pilot, under the guidance of Professor Pedro Gamboa.

Our team is divided into eight secctions:

- **Team Leader** - Afonso Gamboa, 20 years old in the 3^{rd} year, is by far the member with more Air Cargo Challenge knowledge of the team, having closely followed past editions of the competition. He is leading our team with experience, passion and UAV knowledge.

- **Aerodynamics Department** - Diogo Pinho, 20 years old in the 3^{rd} year of the Bachelor's Degree is the coordinator of the aerodynamic design of our aircraft. By his side he has six members: Fernando Faria 3^{rd}, Rodrigo Condeço 2^{nd}, Manuel Pereira 2^{nd}, Joana Sousa 2^{nd}, Nuno Riscado 2^{nd} and João Benzinho 2^{nd}. The team was in charge of the airfoil selection for both the wing and tail, the fuselage optimization and 3D wing optimization.

- **Structures Department** - Beatriz Gonçalves, 20 years old in the 3^{rd} year of the Bachelor's Degree is the coordinator of the structural design of our aircraft and she is also the team Treasurer, handling the team's sponsorships and expenses. By her side she has four team members: Mafalda Assis 3^{rd}, José Barros 2^{nd}, Daniela Pereira 2^{nd} and Gonçalo Coimbra 2^{nd}. With multiple hours in $Ansys$, the team has done the work to make sure that the components will not fail in the flight, from wing sizing, fuselage, tail boom to the wheels.

- **Propulsion Department** - Anton Mamus, 21 years old in the 3^{rd} year of the Bachelor's Degree is the coordinator of the propulsion team. By his side he has five members: Henrique Vieira 3^{rd}, Francisco Ribeiro 3^{rd}, Rafael Andrade 2^{nd}, David Simões 2^{nd}, Dmytro Kovalchuk 2^{nd}. They were in charge of all wind tunnel tests, such as discharge of the battery with multiple propellers, aiming to maximize the propulsive system's efficiency and choose the best propeller for our needs.

- **Eletronics Department** - Miguel Ruívo, 20 years old in the 3^{rd} year of the Bachelor's Degree is the coordinator of the eletronics team. By his side he has two team members: André Sousa 3^{rd} and Diogo Garcia 3^{rd}. They took charge of the study and optimization of all eletronics in the aircraft just like data acquisition systems, servos, battery's and current limiting system.

- **Manufacture Department** - Pedro Leite, 20 years old in the 3^{rd} year of the Bachelor's Degree is the coordinator of the manufacturing in the team. By his side he has two team members: Raul Santos 3^{rd} and Daniel Câmara 3^{rd}. They were responsible for the labor of the UAV, which involved processes such as carbon and glass fiber lamination, mold machining, and various other manufacturing tasks.

- **Marketing Department** - Pedro Moreira, 21 years old in the 3^{rd} year of the Bachelor's Degree is the coordinator of the marketing team. By his side he has two team members: Miguel Albino 3^{rd} and Maria Fernandes 3^{rd}. They were in charge of the social network and public relations, the acquisition of partners and sponsorship's with the goal of expanding the team's network.

- **Pilot** - António Vilaça, a 23 years old in the final year of Integrated Master's Degree, is the person responsible for piloting the aircraft. He is an experienced pilot with Air Cargo experience and has received multiple awards. The team trusts him to deliver the best flight performance of the UAV.

2 Project Management

2.1 Schedule

The project management aims to establish a calendar that includes the deadlines defined by the regulations as well as the dates established by the team for each task. Since this is the first time each member participates in the Air Cargo Challenge, an organised schedule and a review of the work done by the previous teams is important to understand which type of limitations and challenges we might encounter during the project development. So, for the preparation of the Air Cargo Challenge 2024, our team meets once every two weeks to discuss the aircraft development and to help each other. Figure 1 presents the schedule defined for UBI Aeronautics Team to the ACC2024.

The technical report is an important milestone given the fact that at this date the aircraft design must be finished.

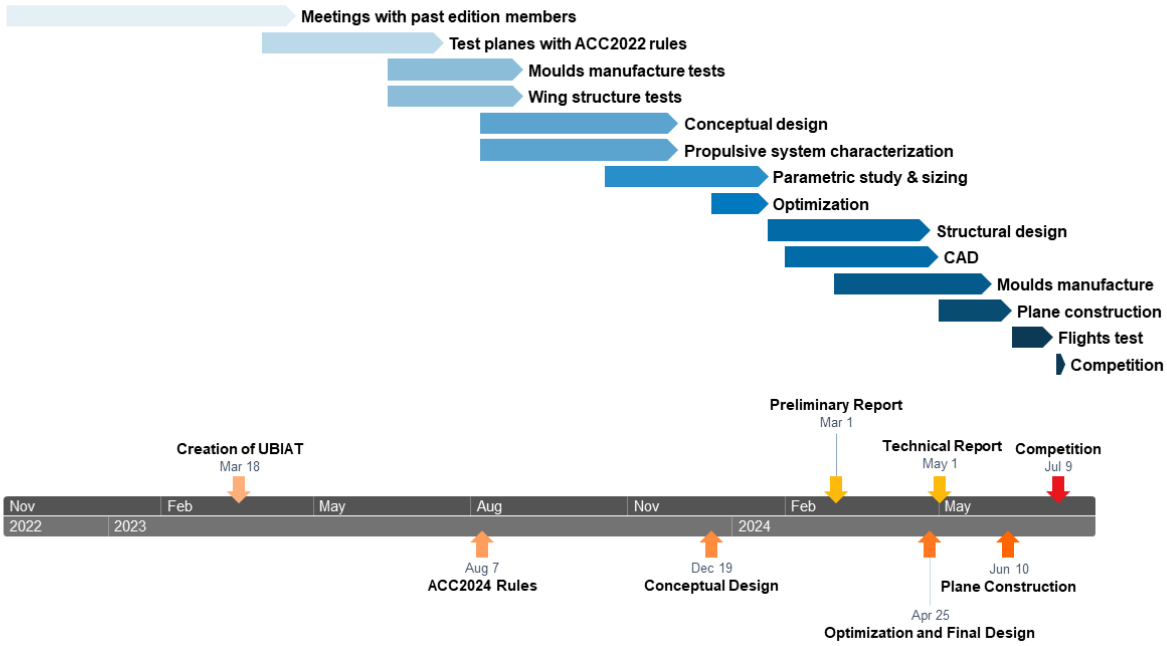

Figure 1: Time schedule

2.2 Sponsors

At the beginning of the project, in january 2023, we had no sponsoring companies and our budget was 0,00€. However, this was never a reason for discouragement. Firstly, we reached the enterprises, showing them our ambition and presenting them with our sponsorship proposal. We received a lot of feedback, some positive, which allowed us to enter in this competition. We should highlight that our first sponsoring entity was AEROUBI & AS COVILHÃ, the Aeronautical Engineering Student Association of the Universidade da Beira Interior.

To this date, we have raised a total of 6538,00€. Due to the geographic positioning of the University, in the interior of the country, the link between the companies and the team is not always easy, since they reside more to the coast side, but we still managed to get the support of some. It should be noted that we had companies that helped us with the support of materials, discounts and the manufacturing of molds.

In the Table 2 can be seen all the companies/institutions that helped us on this journey.

Table 2: Sponsor description

SPONSORS		
Universidade da Beira Interior		1 050,00 €
Reitoria Universidade da Beira Interior		1 000,00 €
Câmara Municipal Da Covilhã		1 000,00 €
Orion Technick - Maintenance & Enginnering		1 000,00 €
COFICAB		615,00 €
AEROUBI & AS COVILHÃ		500,00 €
NAV Portugal		500,00 €
Ricardo & Barbosa		250,00 €
Penedo da Saudade - Suites & Hostel		250,00 €
Relevarte - Arte em Relevo na Madeira		150,00 €
SpaceO		123,00 €
EF Education First		100,00 €
Total Budget		**6 538,00 €**
CEiiA	Manufacture of Wing Molds	
ISQ	Offered Vacuum Pump	
Serra Shopping Covilhã	Gloves, Masks and Brushes	
CN MODELS	50% Discount on al Purchases	
Bilhares Carrinho	50% Discount on al Purchases	
R&G Composite Materials	15% Discount on al Purchases	
Easy Composites	10% Discount on al Purchases	

Figure 2: Sponsors logo

2.3 Financial Outcomes

The table below represents the expenses for the Competition Airplane, Prototype, Construction Materials and Registration/Travel. Therefore, and after all expenses are added together, it is concluded that the expected outcomes of the competition is 7878.94 €.

Table 3: Financial outcomes of the competition

Project Expenses - Competition Airplane	
Wings, Htail, Vtail, Fuselage	
Carbon Fiber (Skin, Web, Cap)	344,70 €
Balsa (Skin, Box, Extra)	50,25 €
Airex	1,69 €
Aramid Fiber Hinge	2,22 €
Plywood	6,40 €
Wheels	20,00 €
Bearings	14,99 €
Steel Rod	2,00 €
Eletronics	
Motor	69,99 €
ESC	24,99 €
Main Battery	19,99 €
RX Battery	5,94 €
Receiver	125,00 €
Servos	420,00 €
Cables	7,58 €
Push Rods	10,62 €
Extras	
Nuts, Bolts, Plugs, Control Horns, ...	40,00 €
Total Expenses - Competition Airplane	**1 166,36 €**
Project Expenses - Competition Construction Materials	
Lamination	
Epoxi Resin	16,59 €
Cups, Brushes, Gloves, Masks	134,13 €
Mould Release, Wax, Microfiber	45,00 €
Peel Ply	174,40 €
Breather/Bleeder Cloth	174,40 €
Vacuum Pump, Bagging Film, Tape	572,55 €
Moulds	
SikaBlock M600	899,70 €
Synthetic Varnish	16,99 €
Steel Rod	8,00 €
Extras	
Sandpaper, Tapes, Glue, Knifes, Rudder Gauge	129,28 €
Total Expenses - Competition Construction Materials	**2 171,04 €**
Project Expenses - Competition Trip	
Registration (300€ per person)	2 400,00 €
Flights Portugal-Germany	560,00 €
Transportation Box Flight Costs - Round Trip	300,00 €
Transportation Box Material	115,18 €
Total Expenses - Competition Trip	**3 375,18 €**
TOTAL EXPENSES - COMPETITION	**7 878,94 €**
(2x Competition Airplanes, 1x Competition Construction Materials, 1x Competition Trip)	

3 Conceptual Approach

3.1 Inicial Design

At the start of our design, we need to understand the mission requirements to approach the problem in the right way. Therefore, special attention was payed to the following parameters:

- the payload (billiard balls) cannot touch each other, meaning a longer fuselage with more aerodynamic drag;
- the motor is predefined, but we can change the propeller, which gives us more versatility in the way we want to approach the problem;
- the runway is made of grass;
- there are 2 flight phases, speed and efficiency;

With all these parameters in mind, some initial ideas where formulated. First we considered using a payload pod, meaning the main fuselage would only take the batteries and the aerodynamic surfaces. That idea was abandoned because with a big amount of payload the pod would be too big and penalize the aerodynamic performance, also due to the organization "Automated Measuring System" we wouldn't be able to place this component in tho pod nor in the small fuselage. Then, for the landing gear, a taildragger configuration was chosen, which can give better performance on the ground. For the tail, there was a indecision between a v-shaped and conventional configuration, but we ended up with the V-tail because of the lower interference drag and the need for only one mold.

3.2 Wing Sizing Process

The sizing processes started by creating an analytical approach, in order to get the wing dimensions for the airplane and then to start the optimization. A relatively complex process was taken to get the most precise results as possible.

That methodology was done for each propeller that we had available and will be described in the following steps:
1. Choose an initial airfoil and its respective aerodynamic coefficients;
2. Create various dimensions (chord and span combinations);
3. Calculate the structure weight based on the maximum take-off weight (MTOW);
4. Give an initial payload weight to calculate the MTOW;
5. Iterate the structure weight with the new MTOW and calculate the take-off distance;
6. Iterate the payload until the take-off distance reaches a given value (60m without bonus and 40m for bonus);
7. Calculate the maximum speed and efficiency speed to get the score function result;
8. After getting the best values, proceed to the airfoil optimization and repeat all the process;

9. Get the final dimensions and keep to the 3D optimization.

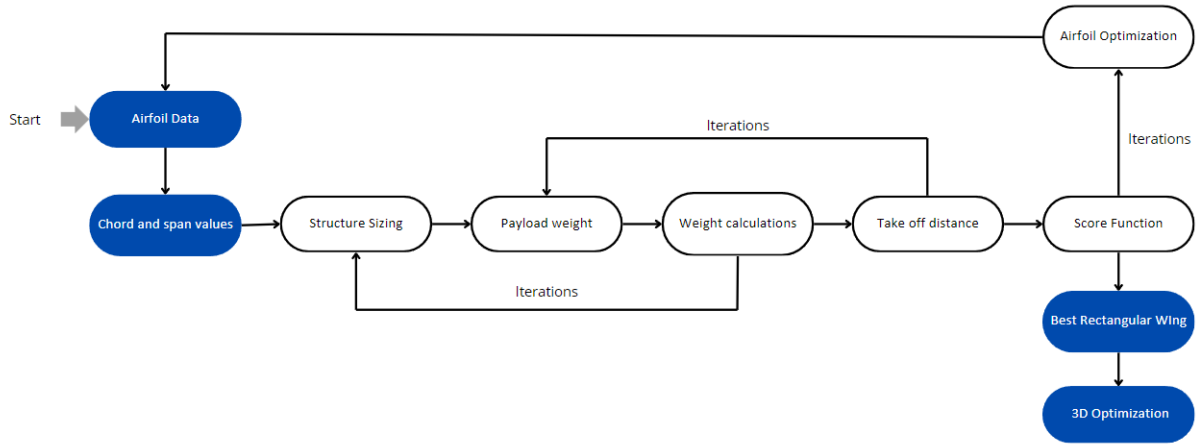

Figure 3: Design process

This process showed in Figure 3 is done for all the thrust curves obtained from the wind tunnel tests. This allowed to choose not only the best dimensions but also the right propeller to get the best scoring.

3.3 Propeller Tests

As this year's competition does not limit the propeller, we first needed to get the thrust curves from different propellers to evaluate their performance and select the one to use.

To do this, we mounted our electric motor with different types of propellers on a wind tunnel balance that provides the acquisition of data like thrust, torque and wind velocity and, knowing the propeller characteristics such as the diameter and the pitch which allowed us to determine efficiency's, with the help of a software, which was designed by a former PhD student, can deduce important values, for example the propulsive system's efficiency.

Figure 4: Wind tunnel hardware

Overall, we tested 12 propellers, some of which where of APC type and the others where Aeronaut CAM Carbon Light. We made tests for different propeller speeds and wind velocities and, obtained graphs that allowed us to compare the results of different propellers. Using the process explained in the previous section, we concluded that the best choice for our project is the Aeronaut CAM Carbon Light 12x6.

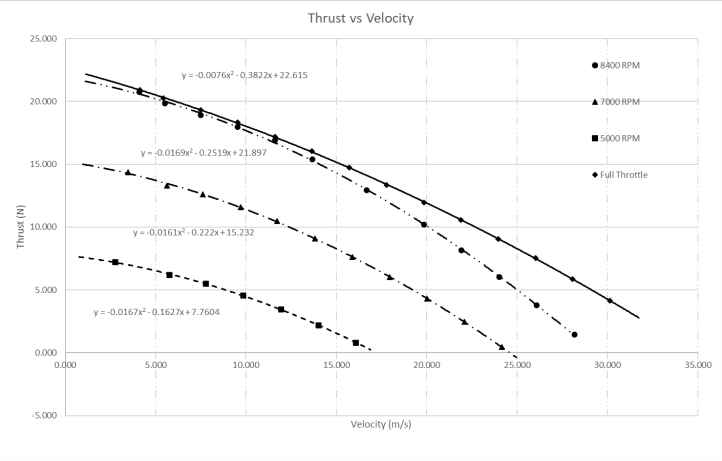

Figure 5: Thrust for different wind velocities for the chosen propeller

3.4 Airfoil Design

Regarding the airfoil selection, collecting airfoils from online databases was the starting point. Then we proceeded to analyse them using XFLR5 for a $R_e\sqrt{C_l} = 198244$, we used this parameter for the analyses because it will be a constant number over the flight phases. This value was obtained using the formula $R_e\sqrt{C_l} = \frac{\rho\bar{c}}{\mu}\sqrt{\frac{W}{\frac{1}{2}\rho S}}$ where the wing area and weight were taken from the previous UBI aircraft from ACC.

To choose the most appropriate airfoil, an objective function has been created paying special attention to the $C_{l_{max}}$, $C_{d_{speed}}$ and $\frac{C_l}{C_d}$. This function weighs specific airfoil characteristics with the best among a large set of airfoils, achieving the best results between flying phases.

$$f = 0.27 \cdot 0.5 \left[\frac{C_{l_{max_i}}}{C_{l_{max}}} + \frac{\left(\frac{C_l}{C_d}\right)_{lo_i}}{\left(\frac{C_l}{C_d}\right)_{lo_{max}}} \right] + 0.19 \left[\frac{\left(\frac{C_l^{\frac{3}{2}}}{C_d}\right)_i}{\left(\frac{C_l^{\frac{3}{2}}}{C_d}\right)_{max}} \right] + 0.27 \frac{\left(\frac{C_l}{C_d}\right)_{max_i}}{\left(\frac{C_l}{C_d}\right)_{max}} + 0.27 \left(\frac{C_{d_{min}}}{C_{d_i}} \right) \quad (1)$$

From the objective function the S4062 airfoil was our initial airfoil, used in the design process. After understanding the aerodynamic requirements that would improve aircraft performance, airfoil optimization was done using inverse design, getting the final airfoil: ”Bacalhau”.

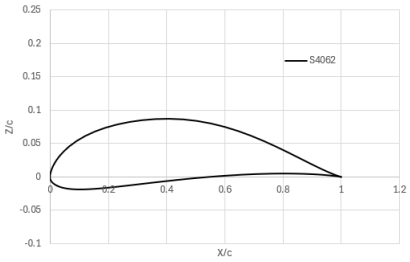

Figure 6: Airfoil S4062

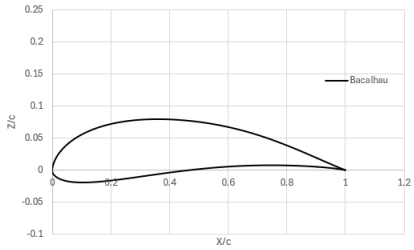

Figure 7: Airfoil ”Bacalhau”

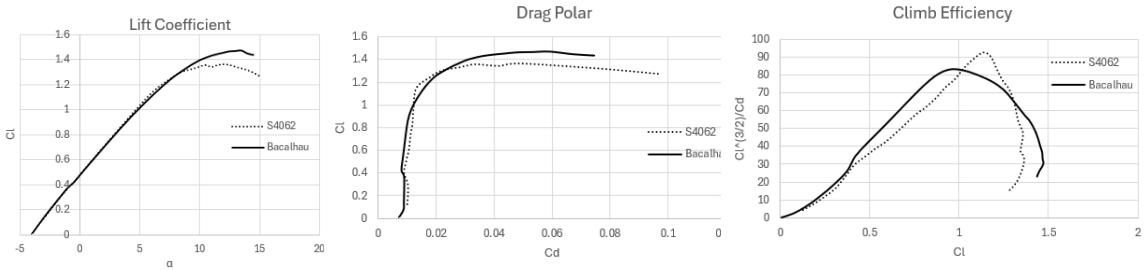

Figure 8: Airfoils polars

From the polars in Figure 8, we can see that the ”Bacalhau Airfoil” has a greater Cl_{max}, less C_d in the speed phase ($0.2 < C_l < 0.3$) and efficiency phase ($0.35 < C_l < 0.5$), but a lower climb rate. As the climb does not count directly to the score, this parameter is not very important, meaning that the optimized airfoil is better than the original.

3.5 Fuselage Optimization

For the fuselage optimization, the starting point was the design of various fuselage geometries which where subsequently analysed using a CFD software. This made us understand the influence of the wing, tail positioning and length on the overall aerodynamic efficiency.

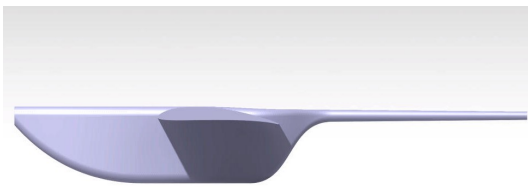

Figure 9: High wing

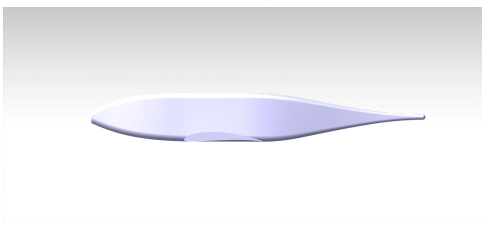

Figure 10: Low wing

In the Figures 9 and 10 we can easily see that two different fuselage lengths are shown (being 0 = short fuselage and 1 = long fuselage) and also two different boom positions in the fuselage (being 0 = middle of the fuselage and 1 = top of the fuselage). Then, it was possible to make a function to

represent the changes in aerodynamic efficiency with the change of these two variables (fuselage length and boom position) and represent the results in a color graphic to choose the best fuselage configuration.

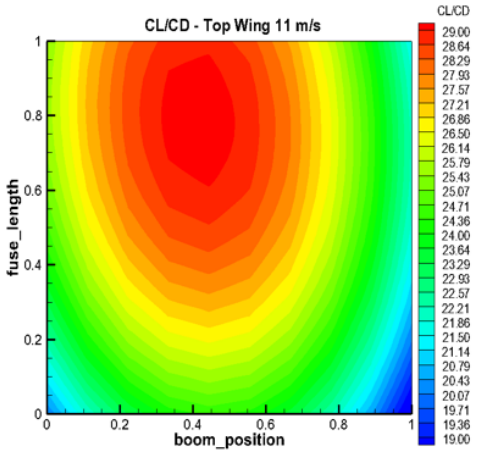

Figure 11: $\frac{C_L}{C_D}$High wing

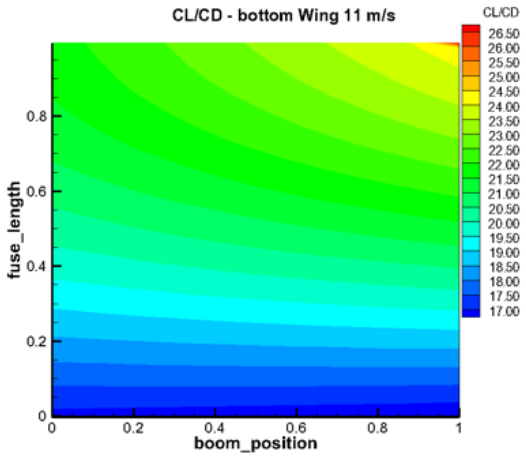

Figure 12: $\frac{C_L}{C_D}$Low wing

With the obtained results, it was possible to choose the high wing configuration as the values for $\frac{C_L}{C_D}$ where bigger. This also could make the airplane more latero-directionally stable and discard the need of putting dihedral in the wing, making it easier to produce. The stability point is discussed in later sections.

3.6 Design Results and Payload

Having all the information about the airfoil, propeller and fuselage, we had everything we needed to do our design process, as mentioned in **section 3.2**. Thus, we where able to choose our wing dimensions and payload weight based on the achieved score.

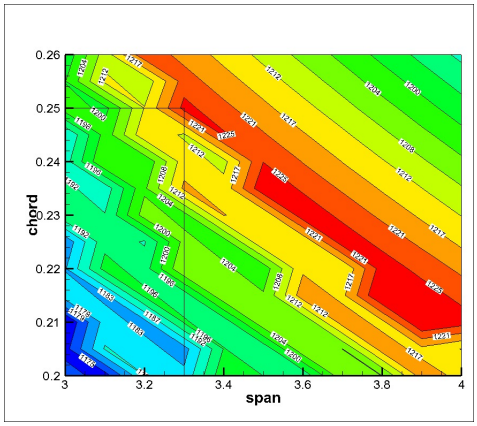

Figure 13: Final design

From the Figure 13 we choose our mean chord as 0.250m and a span of 3.300m, that give us a total wing area of $S = 0.825m^2$. The payload we obtained with our method was 32 billiard balls, which is equivalent to a mass of 5.440kg. We could achieve a larger payload, but then the fuselage would be too long to fit the transportation box, so we chose to have this maximum value. The propeller obtained for this airplane was the Aeronaut CAM Carbon Light 12x6, this could give us a problem because of the maximum current drawn by the motor, but that will be covered in later section.

3.7 Wing Optimization

For the last optimization phase, the XFLR5 tool was used to obtain the drag curves from different wing configurations, such as, rectangular, elliptic, trapezoidal, and rectangular mid panels and elliptical tips. To get the respective dimensions of the wing, the only consideration was that we should have the same wing area as obtained with the design process. The final selected wing layout was the one with rectangular mid panels and elliptic wing tips because of its better lift distribution, which leads to less induced drag, and not so hard to manufacture as a full elliptical wing.

To calculate the root chord, the following procedure was used.

$$\begin{aligned} S_{wing} &= S_{rectangular} + S_{elliptic} \\ S_{elliptic} &= S_{wing} - S_{rectangular} \end{aligned} \tag{2}$$

Having an initial root chord and rectangular span we could calculate the needed elliptic area, and then calculate the chord at the ellipse root.

$$S_{ellipse} = \pi ab \text{ (where } a \text{ is the elliptic span and } b \text{ the ellipse root chord)} \tag{3}$$

As the root chord and chord in the ellipse root are the same we used an iterative calculation to get it. We obtained 0.2735m as our root chord using the rectangular panels span of 0.660m. The tip chord is zero as we use an elliptical configuration.

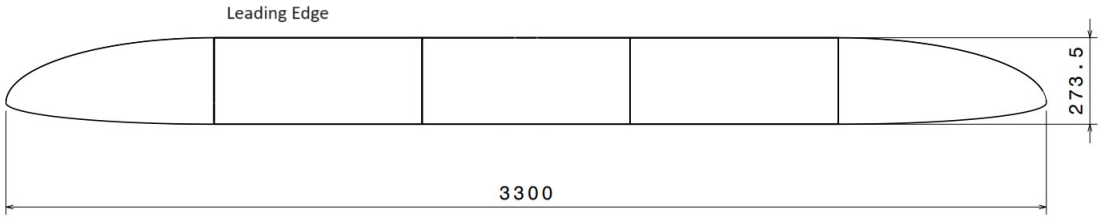

Figure 14: Final wing configuration

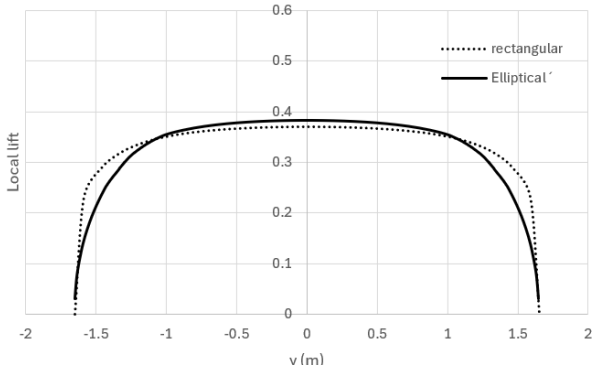

Figure 15: Lift distribution

We can see by the results, that the elliptical wing tip has a better lift distribution, meaning less induced drag. Notice that the aircraft is designed to have a maximum speed of 27.4m/s (CL=0.212) and a efficiency speed of 20m/s (CL=0.398).

4 Stability Analysis

4.1 Tail Design and Static Margin Definition

For the tail calculation, the capabilities of XFLR5 were again exploited, since it can also provide static stability calculations. The V-tail configuration was adopted as mentioned in **section 3.1** and an elliptic format to allow lower induced drag on the tail. The V configuration also made us choose a fully rotating tail, which can lower the drag because no gaps exist on the surface for the rudder-vators.

For the geometry dimensions calculation, first the tail coefficients were defined as:

$$V_h = \frac{l_h S_h}{Sc} \tag{4}$$

$$V_v = \frac{l_v S_v}{Sb} \tag{5}$$

$$S_{vtail} = \frac{\sqrt{S_v^2 + S_h^2}}{2} \tag{6}$$

$$\gamma = \arctan\left(\frac{\frac{S_v}{2}}{\frac{S_h}{2}}\right) \tag{7}$$

where the V_h and V_v are the tail volume coefficients given as 0.5 and 0.029 respectively, the l_h and l_v are the distance between the quarter chord of the wing and the quarter chord of the horizontal and vertical tails, respectively. Knowing the wing dimensions we could calculate the

equivalent vertical and horizontal tails' area and then, the area of each side of the V-tail using the equation (6). Giving an aspect ratio we could get the chord and span of the tail. The dihedral angle was taken from the geometric relation between the horizontal and vertical area getting the value of 37 degrees. The tail volume coefficients were initially different, but after an iterative process it was possible to converge to the mentioned ones.

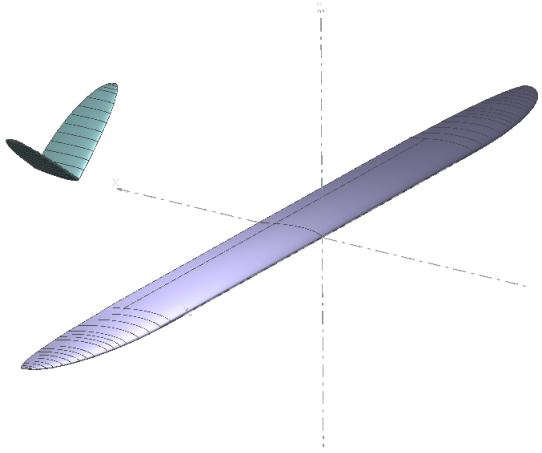

Figure 16: 3D View of aerodynamic surfaces

With the tail geometry finished it was necessary to check the static stability, this is done by getting a positive static margin defined as:

$$ST = \frac{X_{np} - X_{cg}}{mac} \tag{8}$$

where X_{np} is the neutral point position, X_{cg} is the center of gravity position, both starting from the wing leading edge, and mac is the mean aerodynamic chord. As the airplane fuselage is done in a way that the center of gravity won't change if we take out an even number of billiard balls (some from the front of the box and some from behind) as will be explained in later sections, only one cg position was used leading to the results in Table 4.

Table 4: Static stability results

$X_{np}[m]$	$X_{cg}[m]$	mac [m]	ST
0.135	0.1	0.259	12.33

4.2 Laterodirectional Static Stability

The laterodirectional static stability is a combination of two conditions such as lateral and directional. For the lateral motion to be statically stable, $C_{l_\beta} < 0$ is needed, where this factor is mainly influenced by the dihedral angle. As explained before, the wing will have no dihedral but it will be

located in a high position in the fuselage meaning a dihedral effect. This effect was calculated with Eq. (9), (Daniel P. Raymer, Aircraft Design: A Conceptual Approach, 6th edition).

$$C_{l_{\beta_{fuse}}} = -1.2\frac{\sqrt{A}Z_{wf}(D_f + W_f)}{b^2} \tag{9}$$

Using this equation was possible to get an approximation for the C_{l_β} given by the fuselage effect. This way, a dihedral was given to wing in the XFLR5 environment, and the angle was such as the C_{l_β} obtained was equal to the initial plus the calculated one. This showed the dihedral angle to be 0.5 deg.

As for the directional stability, this is more affected by the vertical tail surface. The condition to guarantee static directional stability is $C_{n_\beta} > 0$.

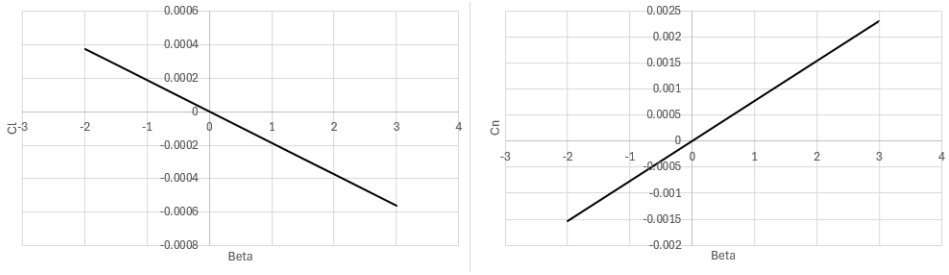

Figure 17: Laterodirectional stability

5 Payload Prediction and cg

Payload prediction is based on our design process, where the span and chord are fixed values and change the air density to get the results. This can show the influence of the air density in payload mass and allow to get the following linear approximation:

$$P = 6.2093\rho - 1.9216 \tag{10}$$

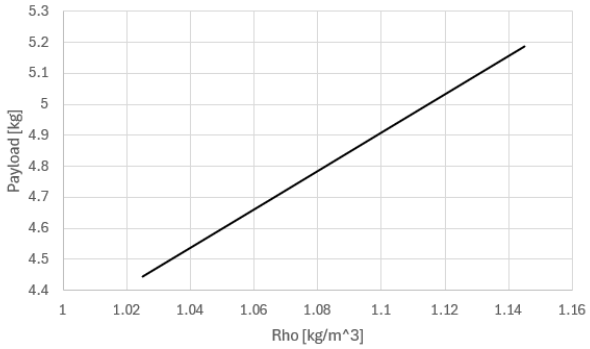

Figure 18: Payload prediction chart

For the cg position, a CAD environment was used. This can have better precision than analytic methods, but takes more time because all aircraft parts need to be designed with extreme detail. The results obtained for the cg position (beginning in the wing leading edge) with payload and without are shown in Table 5:

Table 5: Cg position

Payload mass [kg]	X_{cg} [m]
5.400	0.100
0	0.100

6 Propulsive System

Figure 19 shows the layout for the propulsive system, with the chosen components explained later in this section.

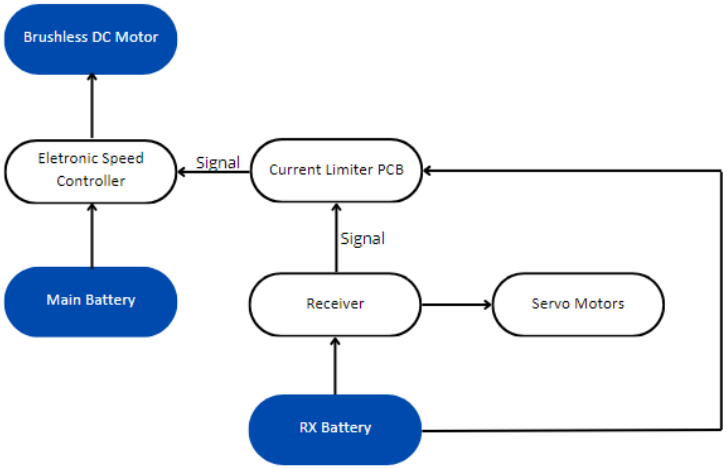

Figure 19: Propulsive system's layout

6.1 Current Penalty

With the introduction of the new current penalty for the time spent above the maximum allowed current of 30 A (Eq. (11)), we decided to run studies to understand how detrimental this penalty would be (Figure 20). Since take-off is made with full throttle and low air speed, with the chosen propeller the penalty would be too high. Given this, we decided to design a PCB that would prevent the current from going above 30 A during the flight.

$$P_{current} = 0.5 \int (I_{current} - 30) dt \tag{11}$$

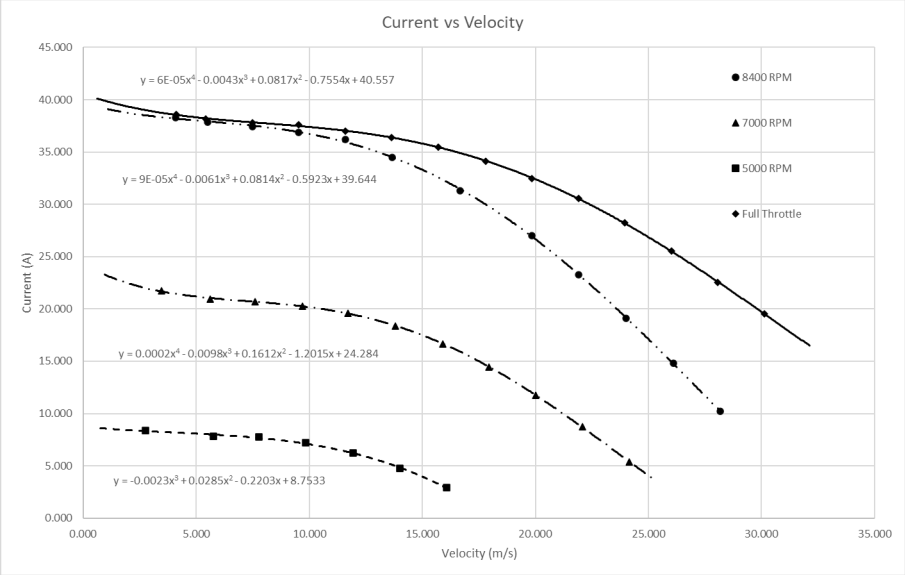

Figure 20: Consumed current for different wind velocities for the chosen propeller.

Currently we are working on two prototypes:

- A 555 timer generating a PWM signal corresponding to 90% of throttle, that is engaged when a current sensor admits the corresponding voltage to a comparator.
- A μC generating a PWM signal corresponding to the correct % of throttle based on the current absorbed by the motor, that is engaged when a current sensor admits the corresponding voltage to it.

6.2 Battery Sizing

Given the weight, size and electrical characteristics of the batteries, we knew that choosing the proper ones was of grand importance to the project. We were also restricted by the competition rules, being the most impactful, the need for the battery to have a minimum discharge rate of at least 40A and a maximum voltage of 12.6V. For the calculation of the capacity of the battery, a time of flight was estimated and the maximum current absorbed by the motor during each of the flight phases, having in consideration a second attempt of take-off and climb, and a safety factor of 50%.

The final value of capacity for the main battery obtained by this method was 3881mAh that was finally rounded to 4000mAh. For the RX battery, after the same calculations, we have landed with a minimal capacity of 335mAh, which is lower than the minimum 600mAh, a value specified by the competition's rules. Besides batteries with higher discharge rate being heavier, they keep the voltage higher during the flight which enables the motor to rotate at higher speeds, and thus, it produces more thrust. This concept was validated with a session in the wind tunnel using the competition's motor and the previously selected propeller, mentioned in **section 3.3**, at full throttle and at an airspeed of 8 m/s, with several 3S baterries with different discharge rates. Finally, the

Flight Phase	Time (s)	Current (A)	Capacity (mAh)
Take-off	18.4 (including 2^{nd} attempt)	30	153.3
Climb	41.6 (including 2^{nd} attempt)	30	346.7
Efficiency	90	30	750
Speed	90	23.1	577.5
Landing (+go around)	120	18	600
Ground	60	2.2	36.7
Total	420	-	2587.4
Safety factor (+50%)	-	-	3881

Table 6: Battery capacity

choice for the main battery was the Turnigy 4000mAh 3S 60C, which weighs around 360g. The RX battery that will by used is the Pichler LiPo Akku LEMONRC 650mAh 2S 35C.

Aiming to maximize the propulsive system's efficiency, we tried to cool the motor with a cooling spray and increase the temperature of the batteries with warm water. Unfortunately, we have not seen any benefits by doing this, so we decided not to use any cooling or warming system.

6.3 Servomotor Sizing

Calculating the integral of the pressure distribution around the control surface, taken from an analysis in XFLR5 with multiple angles of attack, and then dividing by the control surface's span and multiplying by its chord and dynamic pressure, we can get the force applied on the respective control surface. Knowing the position of the point where the resultant force is applied and multiplying by the distance to the control surface's hinge, we get the moment around that hinge. Therefore, depending on the position of the servo inside the wing or the tail, we are able to deduce the required torque of the servo motors.

Below is the equation used to calculate the moment on the control surface's hinge:

$$M = \frac{1}{2}\rho V^2 s \frac{\oint_V p(x)\,dx}{l} \tag{12}$$

where, l is the span of the control surface, s is its chord, ρ is the density of the air and $p(x)$ is the distribution of the pressure on the control surface.

Using this process and multiplying the result by a safety factor of 1.5 we chose the servo KST X08H Plus with a torque of 5.3 $kg \cdot cm$ as the servos to use on our final aircraft.

We are going to use a total of 8 servo motors, 2 for the tail, 2 for the central panel of the wing and the other servos for each of the remaining wing panels.

7 Structural Design

7.1 Wing Structure

The bending load of an aircraft wing is almost carried solely by the wing spar. For calculation purposes it is sufficient to take only the wing spar into consideration.

The wing's root bending moment resulting from lift can be calculated by integrating the lift distribution along the wingspan. A load factor of 3 was used, as mentioned in the regulations. Taking into account the safety factor, a value of 1.5 was applied, as it is a usual value in this area, then a manufacturing factor of 1.25 was also used. This factor is applied due to the fact that we are working with composites.

Integration of the lift along the wingspan b using equation (13) results in the normal force $F_N(y)$ on the wing spar shear web for the flight case. Integration of the normal force along the wingspan using equation (14) results in the spar bending moment. For an exact calculation, the weight of the wing itself has to be considered before integration. This is not necessary in this case because the weight of the wing is negligible compared to the total weight.

$$F_N(y) = \int_{y=-\frac{b}{2}}^{0} n \cdot C_{l,max}(y) \cdot \frac{\rho}{2} v^2 \cdot c(y) dy \tag{13}$$

$$M_b(y) = \int_{y=-\frac{b}{2}}^{0} F_N(y) dy \tag{14}$$

For structural sizing, the maximum values of both load cases at the corresponding spanwise position are relevant. With the known bending moment along the wingspan the wing spar stress σ can be calculated according to equation (15).

$$\sigma_{max}(y) = M_b(y) \frac{Z_{max}(y)}{I_x(y)} \tag{15}$$

Therefore, the second moment of area $I_x(y)$ must be determined. The second moment of area depends on the vertical distance, width, and cross section of the spar flanges. The maximum distance of the spar flanges to the neutral axis is described by Z_{max}. Therefore, the area of the flanges is iterated until the maximum stress is lower than the allowable stress.

The wing torsional stiffness should be as high as possible, otherwise a torsional wing deformation could occur during flight and change the outer wing sections angle of attack and thereby its lift. Additionally, wing flutter could become an issue.

Bredt Batho equation (16) was used to extract the value of shear flow in the shell. This formula is presented below.

$$q = \frac{T}{2A} \tag{16}$$

The wing skin consists of a sandwich made by bidirectional carbon fiber fabric of $11g/m^2$ weight, 1 mm thickness balsa wood and carbon fiber fabric of $11g/m^2$ weight. The carbon fabric has the

fiber oriented at ±45 deg with respect to the wingspan direction, that is in the direction aligned with the torsion moment.

It should be noted that we carried out several analysis and calculations to check which structure was worth using on the wing. Initially we had two options: sandwich structure or foam core structure (XPS). It was found that, in fact, the structure that was lighter on the wing was made of sandwich (carbon fiber + balsa wood).

The spar is a sandwich element, with a layer of $90g/m^2$ carbon fiber, followed by 10mm of Airex and, subsequently, with another layer of $90g/m^2$ carbon fiber. The fiber orientation is ±45 degrees aligned with the wingspan. To glue the spar to the lower surface and upper surface of the wing, microbaloons embedded in epoxy resin are used.

Epoxy resin is used as a matrix for the fabrics and the sandwiches are obtained with the vacuum moulding technique.

The wing is divided into five sections/panels measuring 0.66 m each. To connect these parts, we will have a smaller spar that enters an open space in the main spar, enabling the transmission of the bending moment. There is also a small carbon pin, 3 mm in diameter, located near the trailing edge that allows the transmission of the torsion moment. There will only be ribs in the panel ends and two ribs on the leading edge of the panel that connects to the fuselage in order to hold the pins.

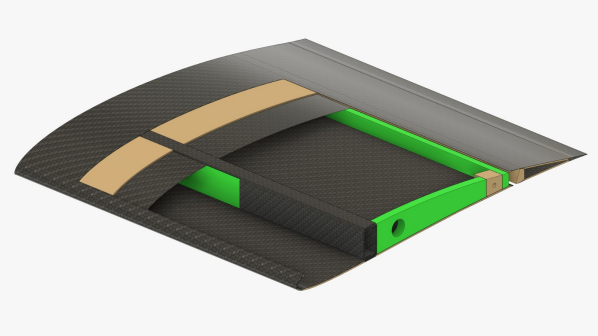

Figure 21: Wing internal structure

7.2 Fuselage and Landing Gears

Regarding the internal structure of the fuselage, it is made up of frames next to the payload opening. Note that the frames are made of 4.2 mm thick plywood. These frames serve to support the plate with the balls. Additionally, there is a frame at the front to support the plate with the electronic components. Also note that among the frames on the plate there is another that contains the frame where the wing will be fixed. The wing is attached to the plate with a screw and the frame gives it stability. The tray in the screw area has $90g/m^2$ carbon to help withstand bending. In the rear area of the fuselage there is a frame where a tube is placed connected to the rearmost frame that serves to fix the tail boom. Finally, there is a smaller 2.2mm frame to join the front part of the fuselage with the rear. There is also a frame for the motor. The structure described is visible in the Figure 22.

It should be noted that, taking into account the structure of the fuselage, 2 layers of $200g/m^2$ carbon fiber and a surface layer of $40g/m^2$ glass fiber will be used.

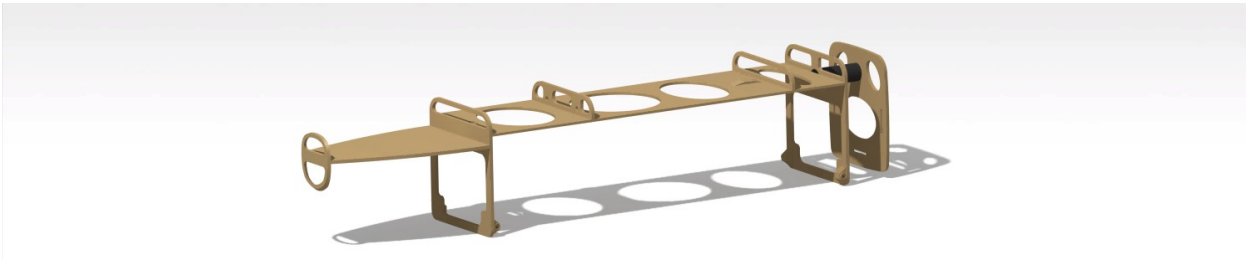

Figure 22: Internal fuselage structure

Regarding the wheels, several analysis were carried out to determine their geometry and dimensions. The wheels have a radius of 50mm, with PLA being used on the inside. From a radius of 40mm outwards TPU flexible filament is used. Figure 23 shows the inside and outside of the wheel, as well as the results of an analysis. It should be noted that in the innermost part of the wheel is located a ball bearing, with 22mm in external diameter, 8mm in internal diameter and 7mm in thickness.

(a) Wheel - Inside view

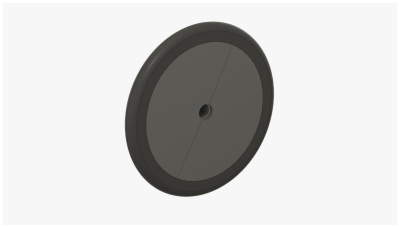

(b) Wheel - External view

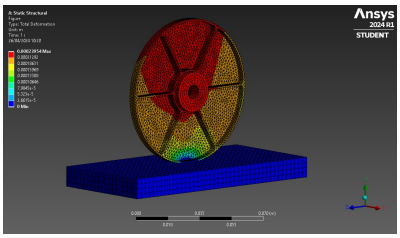

(c) Wheel analysis

Figure 23: Wheel analysis

Regarding the landing gear ”sandwich strut”, we can highlight the structure of the core and faces. Regarding the core, it varies linearly from the center to the tips, containing 12 layers of unidirectional $250g/m^2$ tape in the center. Subsequently, from the center to the tips this weight will be reduced, reaching 8 layers of unidirectional tape $250g/m^2$ at the ends. As for the faces, it also varies linearly from the center to the ends. In the center there will be 4 layers on top plus 4 layers on the bottom of ±45 degrees of $200g/m^2$ woven. This weight will decrease until reaching 2 layers on top, plus 2 layers on the bottom of ±45 degrees of $200g/m^2$ woven on the ends. The geometry of this strut is shown in Figure 24.

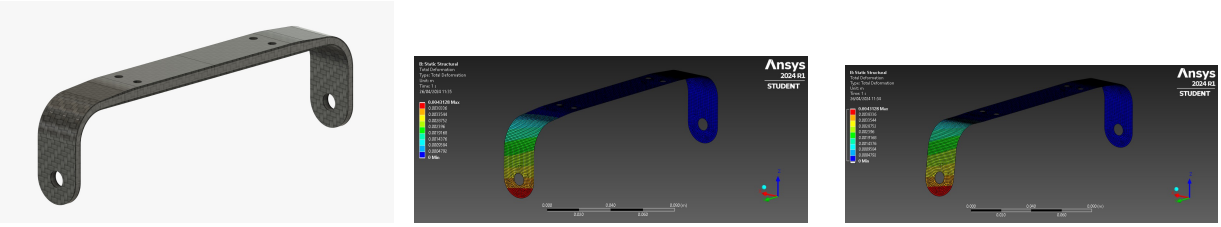

(a) Landing gear strut (b) Without deformation (c) With deformation

Figure 24: Landing gear strut analysis

7.3 Loading System

To have a quick and efficient loading and unloading system we have designed a platform that holds two boxes made of balsa wood with 16 compartments each, to place a total of 32 pool balls.

The platform itself has a sandwich structure with $90\ g/m^2$ woven carbon fiber and Airex foam core with a small inclusion of wood to hold the main landing gear. It has wedge-shaped guides to facilitate the entrance of the boxes into the fuselage and carbon fiber tubes at the ends to hold the platform with the payload to the fuselage with two carbon fiber rods. The entire structure of the loading mechanism was carefully analysed on $Ansys$ to prevent the failure of the structure during the flight and landing phases.

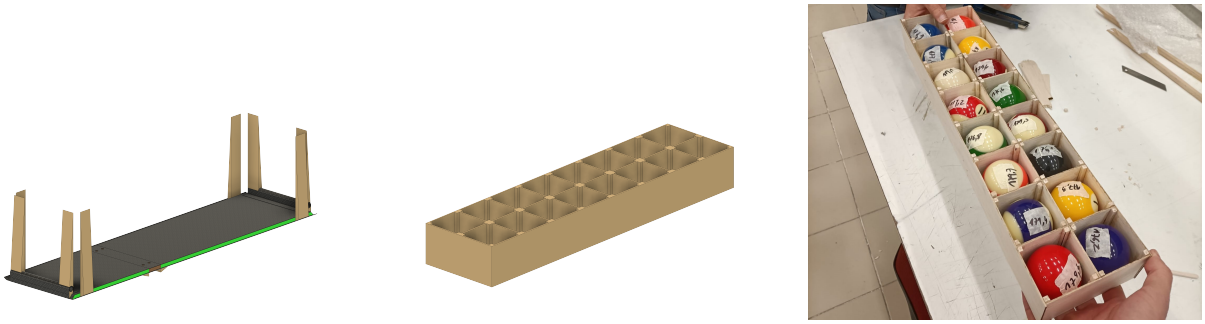

(a) Payload platform (b) Payload box CAD (c) Payload box testing

Figure 25: Loading system design

7.4 V-Tail

Opposite to the wing, in the calculations relating to the choice of the type of structure in the tail, it was found that the lightest structure would be the Foam Core (Carbon + XPS). It should be noted that, in previous tests, it was found that XPS absorbs a lot of resin during the manufacturing process. This indicates that, although these results are more positive for foam core structures (even with the manufacturing factors implemented in the calculations) it was necessary to think about this observation. Therefore, we also chose to use a sandwich structure (carbon fiber + balsa wood) for the tail.

We also had a dilemma between making a hinge on the tail surface or having the entire empennage rotate. It should be noted that, in the prototypes we designed for testing the previous edition, we found that it is really difficult to make a precise manual cut to design the hinge. Furthermore, as the surface is elliptical, it would become even more difficult to do so. Also note that the hinge would create a lot of drag. Therefore, it was decided not to make a hinge on the tails, but rather to have a carbon tube to allow them to rotate. This carbon tube transmits shear and bending to the spar through the ribs.

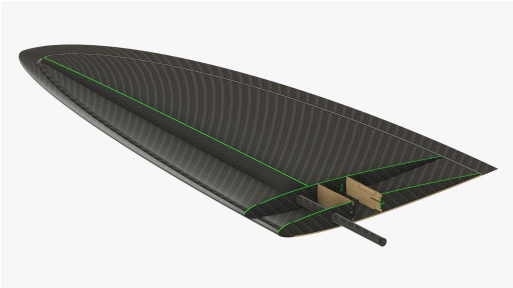

Figure 26: Tail internal structure

Regarding the tail cone structure, the component that connects the fuselage to the tail, will be a constant section tube with the following dimensions: 760mm long, 20 mm external diameter and 19 mm internal diameter. The carbon fiber orientation is 0/90 degrees.

The tail boom is connected to the tail via a carbon support, this support is presented in the Figure 27.

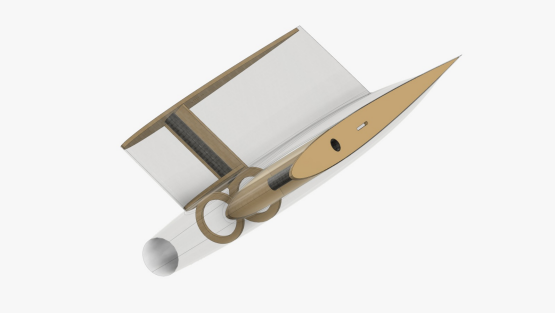

Figure 27: Tail boom and tail connection support

7.5 Airplane Transport Box

The transport box will be made of MDF and will have approximately the following internal dimensions: 800x300x300mm. It should be noted that, eventually, the box may undergo minor changes in its size.

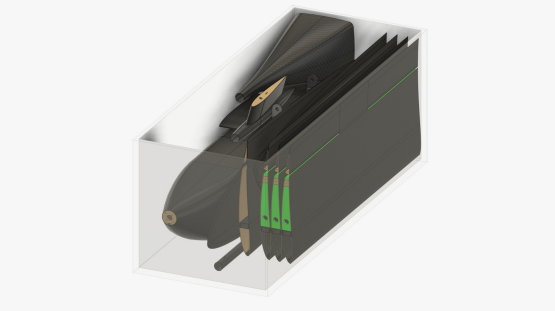

Figure 28: Airplane Transport Box

8 Manufacturing Process

8.1 Prototypes

One of the very first tasks performed by UBIAT was the construction of two prototypes that shared the same fuselage but each with a different wing and tail. The team was split in half and the aircraft's were based on the 2022 Air Cargo Rules. Then the prototypes went to fly in Covilhã's Aeroclub and their performance compared.

Figure 29: Prototypes

This was a learning activity in which the team began to understand the design process and to develop manufacturing skills that would be necessary for the months that followed. The airplanes were made in a cheap way and the perfection and detail were not our main concern, however the real purpose was to start the "Air Cargo Process".

8.2 Tests

The hand lay-up processing technique was the next task performed by the team, so we started producing possible wing sections with 200 g/m^2 carbon fiber. This was our first contact with composites and we used the tests to figure out which option were better to our final wing: sandwich shell with a carbon-Airex spar or a sandwich shell with a XPS Foam core. The latter revealed itself lighter, however as it was porous it was difficult to find grip between the core and the shell, also the lack of a spar made this method less rigid. As the weight difference was not so big, we selected the wing with carbon-airex spar.

These tests served also as a tryout to our vacuum machine and helped learn with the mistakes on the vacuum bag cutting, resin and hardener portions, timming, quantities and also a more effective fiber cutting technique.

(a) XPS foam core

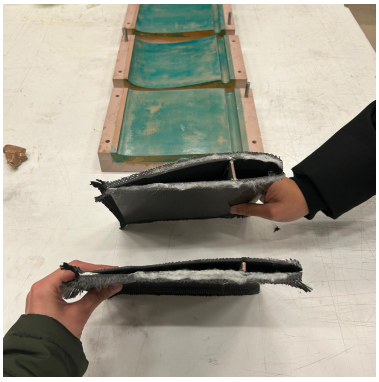

(b) Carbon-Airex spar

(c) Vacuum tests

Figure 30: First lamination tests

Multiple ways and products to the release of the laminated part were tested:

- PVA
- wax
- wax and PVA
- PVA and wax

The team concluded that the best way was to only use the wax.

For the next step the team wanted to go deeper, to obtain a more professional result and to prove that the empennage mechanism would work, so the the tests were made in two ways. The first one with $60g/m^2$ woven glass fiber didn't went so well because it was our first time laminating with this type of fiber and we noticed a lack of resin, but it served to prove the mechanism was efficient. The second test with $20g/m^2$ bidirectional carbon fiber went perfect and we also managed to paint the team's number on it.

These tests were a success, since the finishing of the fiber was good and even more importantly the tail mechanism worked very well.

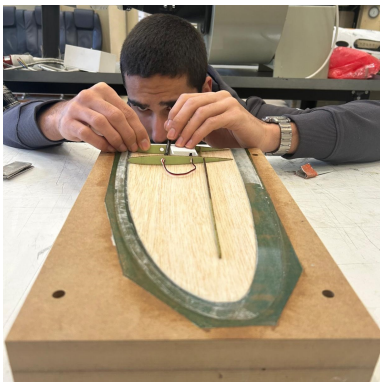

(a) Glass fiber test

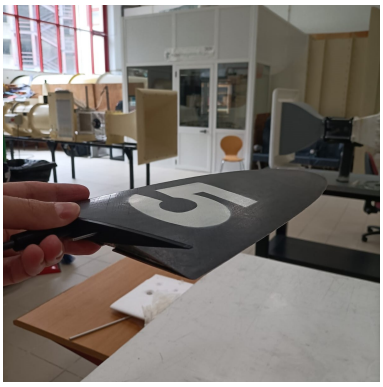

(b) Carbon fiber test

Figure 31: Empennage tests

With the *Ansys* analysis in sight, the manufacture department's work was to obtain the elastic modulus, *E*, to use it in the computacional program to perform the analysis of the internal fuselage structure. A strength test was carried out on plywood samples until failure.

(a) Plywood sample test

(b) Plywood broken

Figure 32: Plywood tests

The material strength tests did not stop there and we continued with the wheel tests. First, a total of six different wheels were made to do tryouts to their hardness, weight and reliability. The six wheels were divided by three different diameters (60mm, 80mm and 100mm) and then two different thickness of each diameter (8mm and 12mm).

A rudimentary structure was built to sustain the aircraft weight and fix the wheels right underneath was developed. Then we took the wheels to the local AirClub field and tested every wheel in different types of grass and dirt.

We got to the conclusion that the weight difference added by the 12mm width was not justified by the hole oppened to the ground, so the 8mm thickness was selected, but we will also take the 12mm width wheels in case the terrain is soft or wet. Also the tests revealed that for this type of fields the 60mm diameter wasn't enough and between the 80mm and 100mm the team selected the larger diameter one because it would provide a safer ride on the ground.

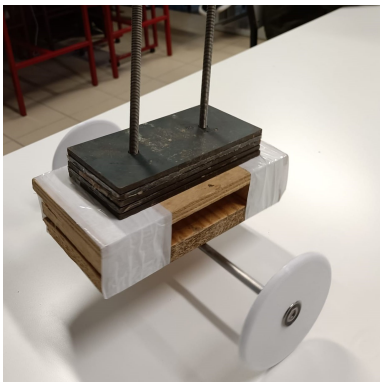

(a) Initial wheels test

(b) Final wheel tests

Figure 33: Wheel tests

The wheels' dimensions being settled, the team started the development and its composition was already explained in **section 7.2**. Strength tests were made and we figured out that a single wheel could carry 400N, that is way beyond the final aircraft weight, so there is no risk of the wheels failing.

8.3 Wing and Tail Surfaces

The wing molds were developed in the university using the software *Autodesk Fusion 360* and then were sent to our partner CEiiA in Porto to be produced. This wing central moulds will be used to manufacture the three rectangular panels per wing which means that they will produce six moulds.

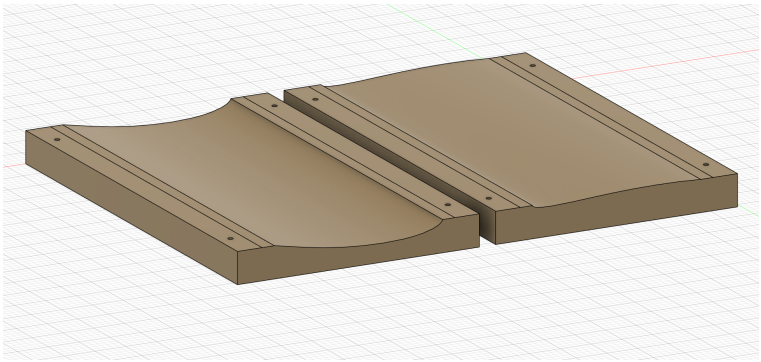

Figure 34: Wing central molds

The real challenge in the design of the molds was the asymmetries in the mold tip. That is because in order to make the elliptical form with a straight upper surface of the wing it is required that the lower surface has a dihedral. The team had to start right in the *CATIA* CAD because it was difficult and more effective than it was in *FUSION 360*.

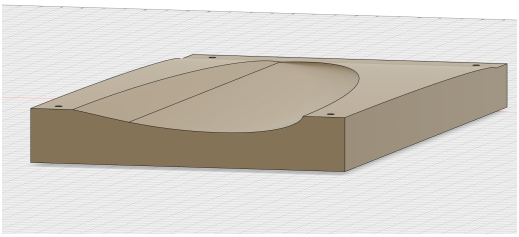

(a) Lower surface with dihedral

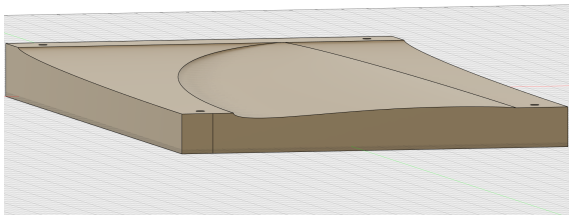

(b) Straight upper surface

Figure 35: Tip of the wing molds

The tail surfaces molds were easy and fast to fabricate because of its symmetric shape. Developed in *FUSION 360* and then machined on the department's CNC machine with 10mm flat, 6mm flat and 3mm ball milling cutters. This produced single SIKA BLOCK M700 mould, wich will be used to fabricate the four tail surfaces as the moulds re-usability is one of the V-Tail advantages

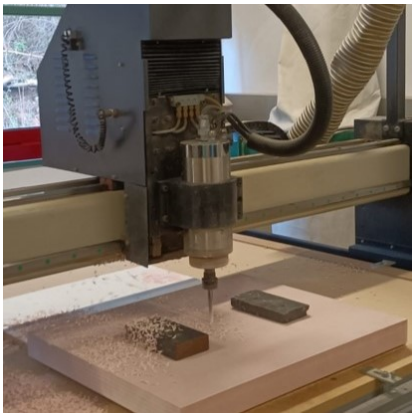

(a) Department's CNC machine

(b) Final tail surfaces moulds

Figure 36: Tail surfaces moulds

8.4 Fuselage

In order to avoid subsequent and imprecise cuts on the wing and loading tray, the fuselage moulds already include gaps where it will be possible to laminate and avoid this positions. Also, as the fuselage is more than 80cm long, it was divided in two.

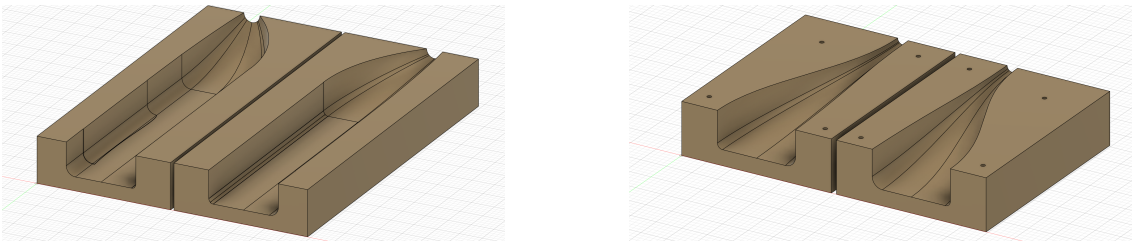

(a) Front fuselage moulds

(b) Rear fuselage moulds

Figure 37: Fuselage moulds

9 Outlook

With this technical report, we intend to show the jury that we are a team able to achieve good results since we gave the best we could with the strict agenda available. It was a little difficult to organize ourselves since a vast part of our team members are in the last year of aeronautical engineering bacheler's degree, which is the most time consuming and exhausting year of studies.

Throughout the aircraft development process, we encountered a wide range of challenges, since Universidade da Beira Interior is located in an underdeveloped region with difficult access to materials and potential sponsorships. This required us to order the majority of materials and endure lengthy waiting times. Therefore, efforts to secure sponsorships and promote the team and our project had to be intensified to ensure it did not compromise the team's work development in any way.

Despite all the hurdles faced, the team believes in our aircraft potential to deliver notable performances and stand out in various competition parameters.

In the next few weeks there will be times of hard work, patience and precision. With around a third of the moulds made, the team will split in a way so that the work is more fluid and the stages of manufacture do not become dependent on each other in the event of shortages or delays in material delivery. The team is ready and completely focused on the project as our result will be a mirror of our commitment.

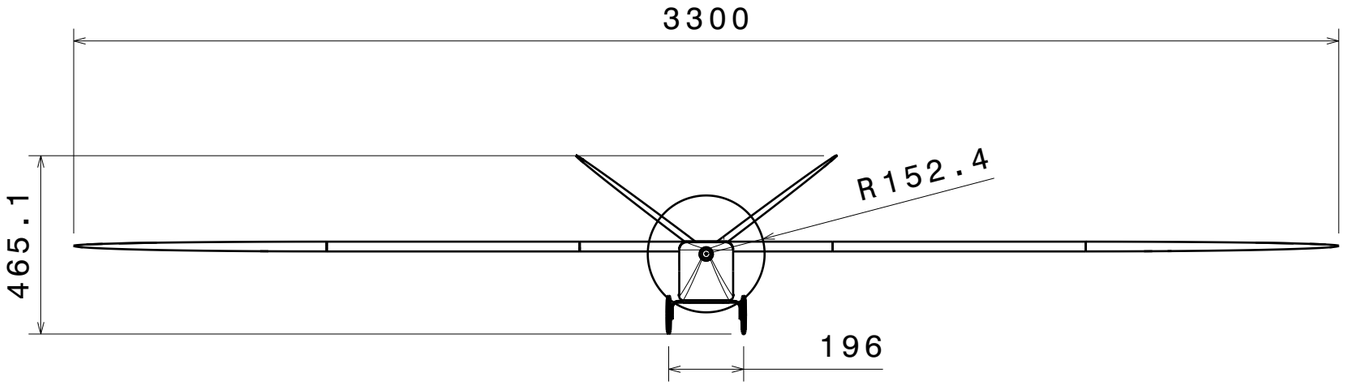

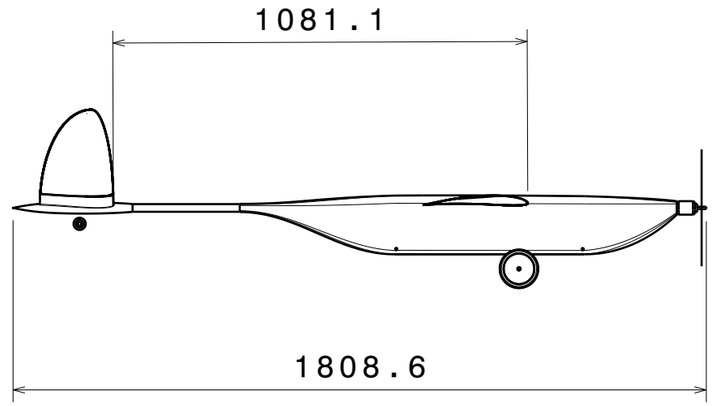

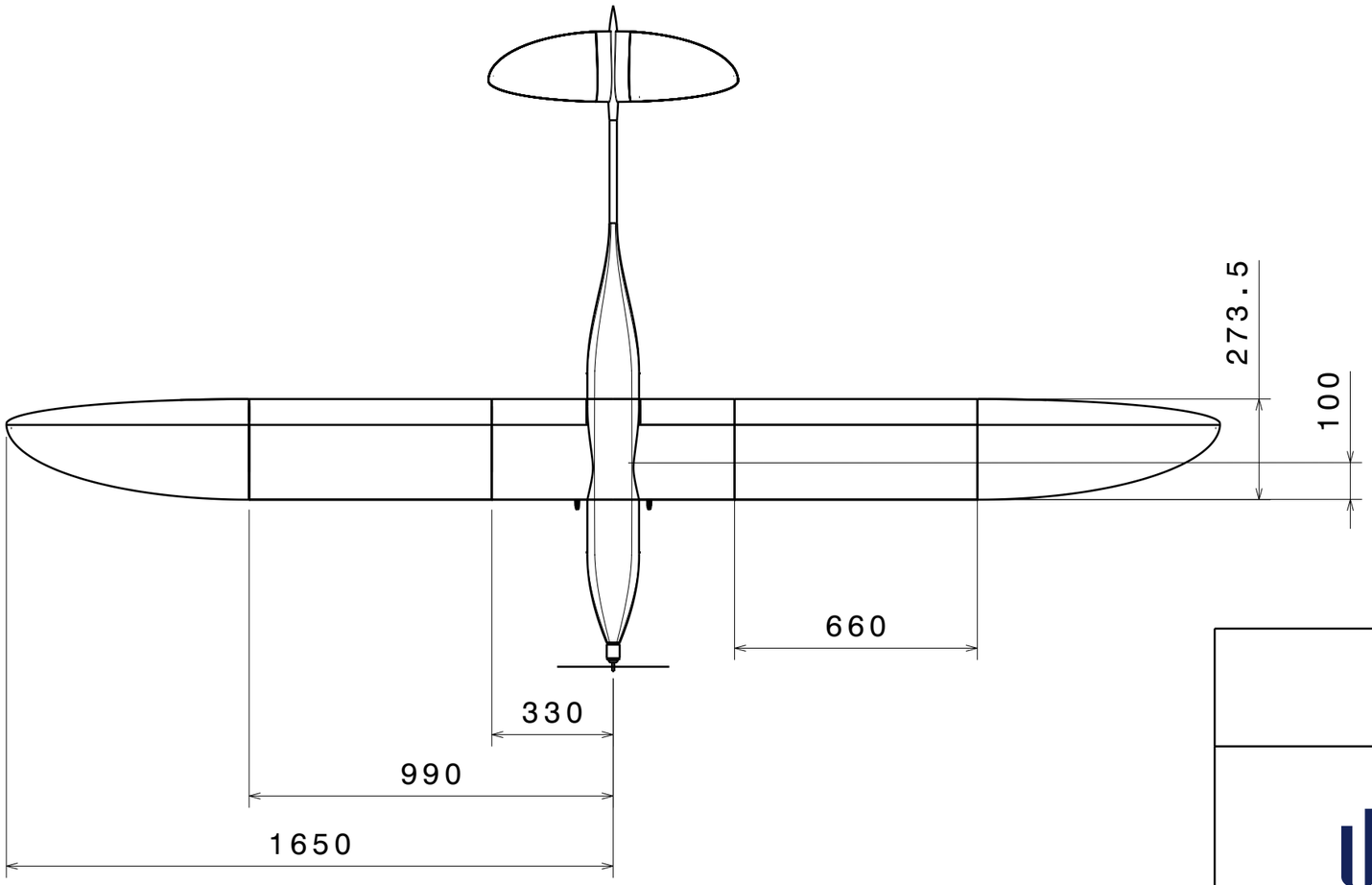

wing span	3300 mm
wing root chord	273.5 mm
wing mean chord	250 mm
wing area	0.825 m^2
wing aspect ratio	13.2
angle of setting wing	+1 deg
empennage span	415 mm
empennage root chord	192 mm
empennage mean chord	150 mm
empennage area	0.063 m^2
empennage dihedral	106 deg
center of gravity	100 mm

3-view drawing

UBIAT
Team 05

Author: UBI Aeronautics Team

Date: 30/04/2023

Scale 1:16

SIZE A3

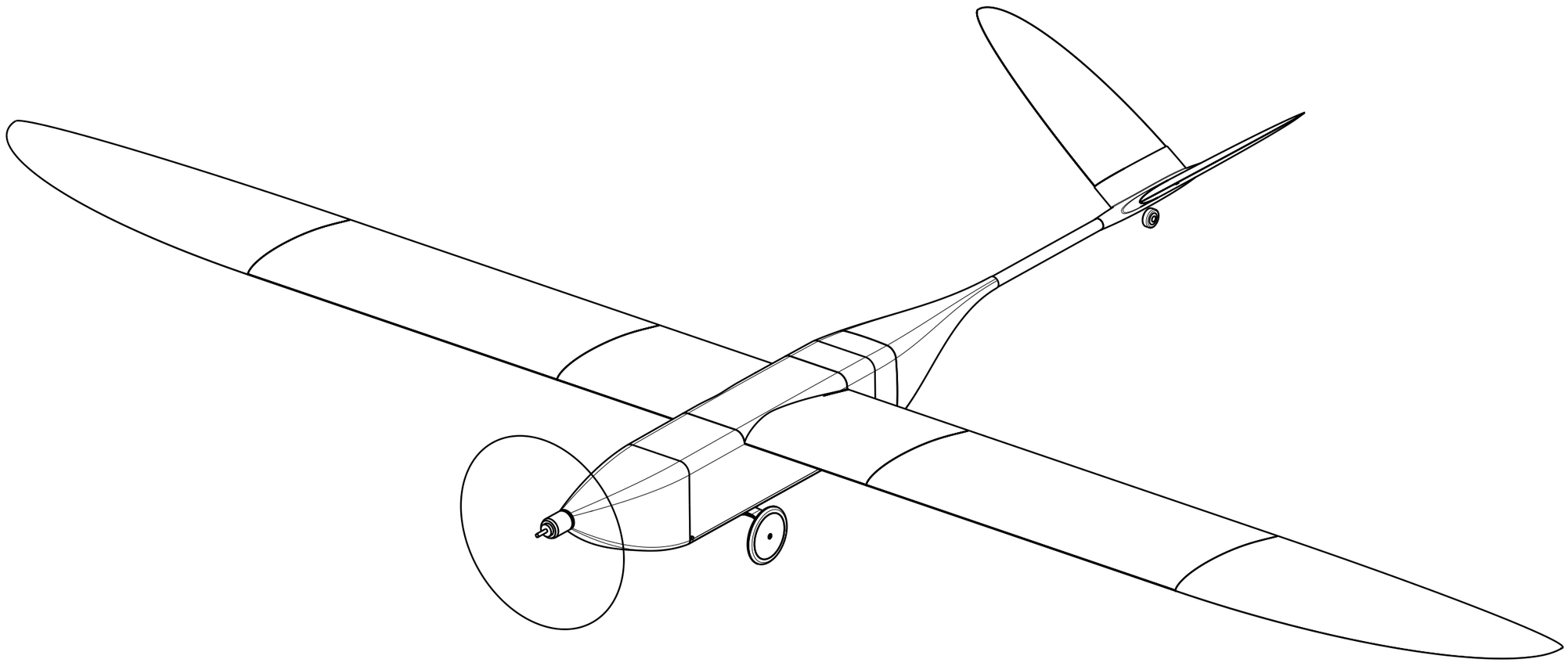

Isometric view

UNIVERSIDADE BEIRA INTERIOR

UBIAT
Team 05

Author: UBI Aeronautics Team

Date: 30/04/2023

Scale 1:8

SIZE A3

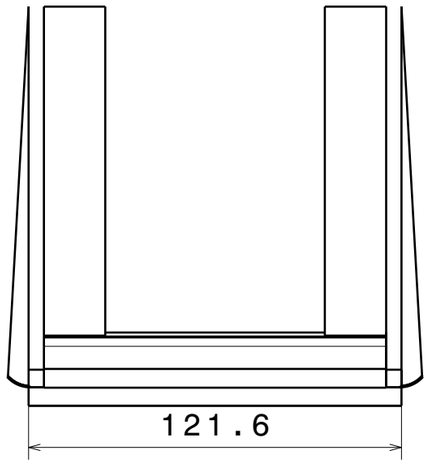

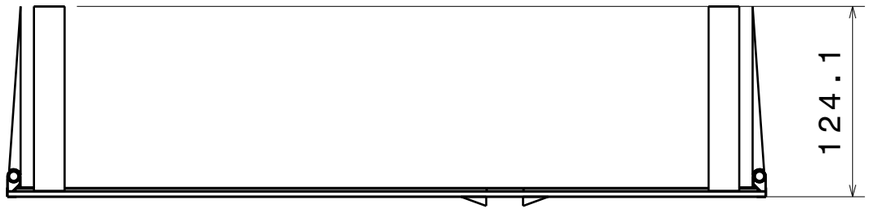

Left view
Scale: 1:4

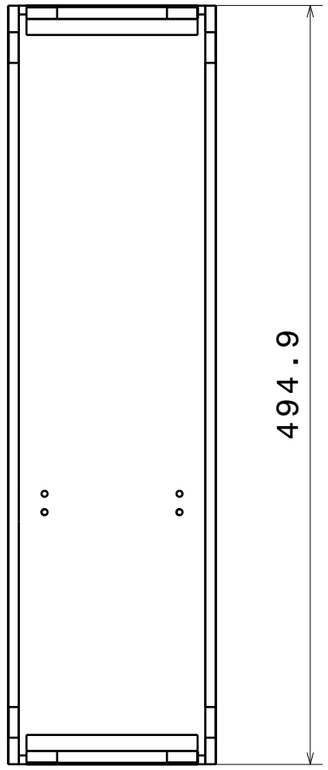

Top view
Scale: 1:4

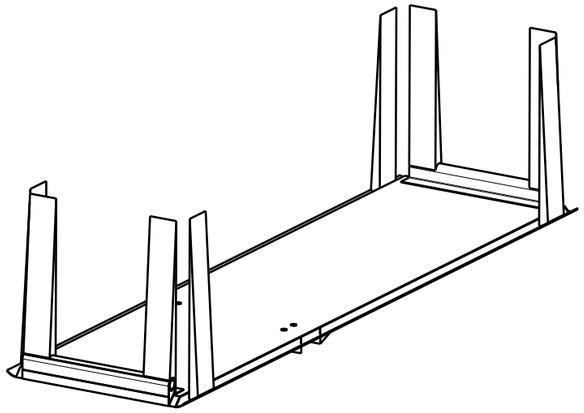

Isometric view
Scale: 1:4

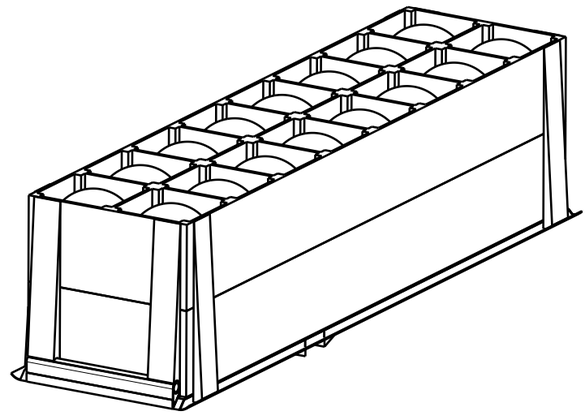

Isometric view
Scale: 1:4

Note:Board and Payload

Payload board

UNIVERSIDADE BEIRA INTERIOR

UBIAT
Team 05

Author: UBI Aeronautics Team

Date: 30/04/2023

Scale 1:2

SIZE A3